Proceedings of the 6th International Conference on the Application of Physical Modelling in Coastal and Port Engineering and Science (Coastlab16)

Ottawa, Canada, May 10-13, 2016

MODEL OF SOLITARY WAVE OVER BED RISING USING NAVIER STOKES EQUATIONS WITH MAPPING TECHNIQUE

ALIREZA LOHRASBI[1], MOHARRAM D. PIROOZ[2], ALIREZA LAVAEI[1]

1 Department of Civil engineering, College of engineering, Boroujerd Branch, Islamic Azad University, Iran

Email: ar_lohrasbi@yahoo.com

2 Associate Professor, School of Civil Engineering, College of Engineering, University of Tehran, Tehran, Iran

Email: m_dolat@ut.ac.ir

ABSTRACT

This article concerns a solitary wave propagating over a rising bed assuming unsteady, incompressible viscous flow with free surface. The method solves the two dimensional Naiver-Stokes equations for conservation of momentum, continuity equation, and full nonlinear kinematic free-surface equation for Newtonian fluids, as described by the governing equations in a vertical plan. A mapping was developed to trace the deformed free surface by transferring the governing equations from the physical domain to a computational domain. Finally a numerical scheme is developed using finite element modelling technique to predict the flow over a rising bed with using the Arbitrary Lagrangian Eulerian algorithm. The results compare well with other research and results showsare generally favorable.

KEYWORDS: Solitary wave, Rising bed, Naiver-Stokes equations, Mapping.

1 INTRODUCTION

Understanding the effect of waves and coastal bathymetry is difficult but very useful in protect coastal areas from storm wave attacks. Hydrodynamic processes in the coastal region are very important factors for coastal engineering design, in which the water wave propagation and its effects on coasts and on the coastal structures are extremely important. Tsunamis are more dangerous in shoreline and it was developed various measures to reduce tsunami damage. One of the tsunami protections is submerged breakwaters. Two-dimensional experiments on wave transmission on bed rises such as submerged breakwaters have been carried out by previous researchers the application of the results to particular coastal protection projects is difficult and inapplicable in many cases. Solitary waves usually used to represent for both tsunamis and extreme design waves.

There have been many researchers who have studied and written numerous papers about the free surface problems and its shape over bed rises. Wellford and Ganaba(Wellford & Ganaba, 1981) analyzed free surface problems involving free surface motions using finite element techniques. Kim et al.(Kim, Liu, & Liggett, 1983) used the Boundary Integral Equation Method (BIEM) for the same problem. Some numerical studies of breaking waves have been dominated using two-dimensional potential flow methods by Dommermuth et al.(Dommermuth et al., 1988). This method works on irrotational and incompressible flow assumptions and has no viscous effects. Ramaswamy and Kawahara(Ramaswamy & Kawahara, 1987) adopted an Arbitrary Lagrangian-Eulerian description to solve free surface flow involving large free surface motion using finite element techniques. Cooker et al.(Cooker, Weidman, & Bale, 1997)studied on the numerical solutions for fully nonlinear two-dimensional irrotational free-surface for the interaction between a solitary wave and a submerged semicircular cylinder with using Laplace's equation. Hayashi et al.(Hayashi, Hatanaka, & Kawahara, 1991) applied a finite element analysis on the Lagrangian description, combined with a fractional step method to solve unsteady incompressible viscous fluid flow governed by Navier-Stokes equations. Lemos(Lemos, 1992) solved the unsteady flow equations and updated the free surface in time using the volume of fluid method and modelled turbulence using the k—e closure equations. Dolatshahi and Wellford(Dolatshahi P. & Wellford, 1995) analyzed free surface profile with a two dimensional

Arbitrary Lagrangian-Eulerian finite element method. Zhou and Stansby (Zhou & Stansby, 1998) extended an Arbitrary Lagrangian-Eulerian model in the σ coordinate system (ALE σ) for shallow water flows, based on the unsteady Reynolds-averaged Navier-Stokes equations. Gaston and Camara (Gaston & Kamara, 2000) presented a two-dimensional Lagrangian-Eulerian finite element approach for non-steady state turbulent fluid flows with free surfaces. Lo and Young (Lo & Young, 2004) described the application of velocity-vorticity formulation of the Navier-Stokes equations for two-dimensional free surface flow using an arbitrary Lagrangian-Eulerian method. Christou et al (Christou, Swana, & Gudmestad, 2008) studied on the behaviour of nonlinear regular waves interacting with rectangular submerged breakwaters. A new series of experimental results is presented and compared with numerical calculations based upon a Boundary Element Method (BEM) that utilises multiple fluxes to deal with the discontinuities encountered at the corners of the domain. Irtem et al.(Irtem, Seyfioglu, & Kabdasli, 2011)investigated the effect of submerged breakwaters on tsunami run-up height as experimentally model.

For the present study, the flow is assumed to be viscous and incompressible. The equations of conservation of momentum and mass for incompressible Newtonian fluids given by Navier-Stokes, and continuity equation along with full nonlinear kinematic free surface equation, are adopted as the governing equations. A particular mapping technique is used to transform the fluid region and its boundaries into a regular geometry for a convenient treatment of the moving free surface and irregular bottom topography. This leads to transformation of the governing equations and the boundary conditions into more complicated equations. However, the transformed equations can be effectively handled by a proper analytical and numerical procedure.

2 PROBLEM FORMULATION

Figure 1 determines the shape of its free surface during the early stages of the process. The physical domain $\overline{V}$ surrounded by a piecewise smooth boundary $\overline{S}$. This domain is occupied by a viscous incompressible fluid with the coefficient of constant kinematic viscosity of ν and the specific mass of ρ.

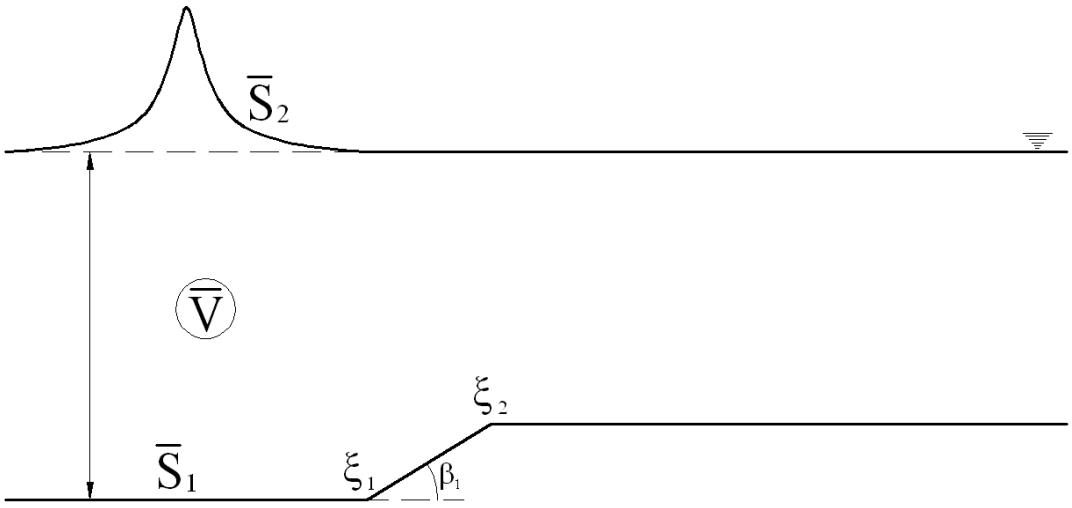

Figure 1. Solitary wave over bed rise

Two dimensional flow with unsteady incompressible viscous is considered. The governing equations are expressed by the unsteady Navier-Stokes equations and the equation of continuity. Let the rectangular coordinates be denoted by x, y and the corresponding velocity components be denoted by u,v. As a result, the equations of conservation of momentum and mass, for incompressible Newtonian fluids, in the arbitrary Lagrangian-Eulerian form are given as follows:

$$\begin{aligned}
&\frac{\partial \bar{u}}{\partial \bar{t}}\Big|_{\xi,\eta} + (\bar{u}-\bar{w}_u)\frac{\partial \bar{u}}{\partial \bar{x}} + (\bar{v}-\bar{w}_v)\frac{\partial \bar{u}}{\partial \bar{y}} = -\frac{1}{\rho}\frac{\partial \bar{p}}{\partial \bar{x}} + \bar{\nu}\left(\frac{\partial^2 \bar{u}}{\partial \bar{x}^2} + \frac{\partial^2 \bar{u}}{\partial \bar{y}^2}\right) \\
&\frac{\partial \bar{v}}{\partial \bar{t}}\Big|_{\xi,\eta} + (\bar{u}-\bar{w}_u)\frac{\partial \bar{v}}{\partial \bar{x}} + (\bar{v}-\bar{w}_v)\frac{\partial \bar{v}}{\partial \bar{y}} = -\frac{1}{\rho}\frac{\partial \bar{p}}{\partial \bar{y}} + \bar{\nu}\left(\frac{\partial^2 \bar{v}}{\partial \bar{x}^2} + \frac{\partial^2 \bar{v}}{\partial \bar{y}^2}\right) - \bar{g} \\
&\frac{\partial \bar{u}}{\partial \bar{x}} + \frac{\partial \bar{v}}{\partial \bar{y}} = 0
\end{aligned} \tag{1}$$

Where w_u and w_v are the mesh velocities in x and y directions. The boundary $\overline{S}$ consists of two types of boundaries: one is the $\overline{S}_1$ on which velocity is given; the other is the free surface boundary $\overline{S}_2$ on which the surface force is specified.

The boundary conditions can be expressed as the followings:

$$\begin{aligned} &\bar{u}=\hat{\bar{u}} \quad on \quad \bar{S}_1 \quad (-\frac{1}{\bar{\rho}}\bar{p}+2\bar{\nu}\frac{\partial\bar{u}}{\partial\bar{x}}).n_{\bar{x}}+\bar{\nu}(\frac{\partial\bar{u}}{\partial\bar{y}}+\frac{\partial\bar{v}}{\partial\bar{x}}).n_{\bar{y}}=\hat{\bar{c}}_x \quad on \quad \bar{S}_2 \\ &\bar{v}=\hat{\bar{v}} \quad on \quad \bar{S}_1 \quad \bar{\nu}(\frac{\partial\bar{u}}{\partial\bar{y}}+\frac{\partial\bar{v}}{\partial\bar{x}}).n_{\bar{x}}+(-\frac{1}{\bar{\rho}}\bar{p}+2\bar{\nu}\frac{\partial\bar{v}}{\partial\bar{y}}).n_{\bar{y}}=\hat{\bar{c}}_y \quad on \quad \bar{S}_2 \end{aligned} \tag{2}$$

where the superscript caret denotes a function which is given on the boundary and n_x and n_y symbolize the direction cosines of the outward normal to the boundary with respect to coordinate x and y. Above Equations can be rendered dimensionless by introducing the following variables:

$$\bar{x}=x\bar{d},\bar{y}=y\bar{d},\ \bar{p}=p\bar{\rho}\bar{g}\bar{d},\bar{u}=u(\bar{g}\bar{d})^{1/2},\bar{v}=v(\bar{g}\bar{d})^{1/2},\bar{t}=t(\frac{\bar{d}}{\bar{g}})^{1/2} \tag{3}$$

Using these transformations, the Equations are modified as follows:

$$\begin{aligned} &\frac{\partial u}{\partial t}\Big|_{\xi,\eta}+(u-w_u)\frac{\partial u}{\partial x}+(v-w_v)\frac{\partial u}{\partial y}=-\frac{\partial p}{\partial x}+\frac{1}{\mathrm{Re}}(\frac{\partial^2 u}{\partial x^2}+\frac{\partial^2 u}{\partial y^2}) \\ &\frac{\partial v}{\partial t}\Big|_{\xi,\eta}+(u-w_u)\frac{\partial v}{\partial x}+(v-w_v)\frac{\partial v}{\partial y}=-\frac{\partial p}{\partial y}+\frac{1}{\mathrm{Re}}(\frac{\partial^2 v}{\partial x^2}+\frac{\partial^2 v}{\partial y^2})-1 \\ &\frac{\partial u}{\partial x}+\frac{\partial v}{\partial y}=0 \end{aligned} \tag{4}$$

And Boundary conditions are:

$$\begin{aligned} &u=\hat{u} \quad on \quad \bar{S}_1 \quad (-p+\frac{2}{\mathrm{Re}}\frac{\partial u}{\partial x}).n_x+\frac{1}{\mathrm{Re}}(\frac{\partial u}{\partial y}+\frac{\partial v}{\partial x}).n_y=\hat{c}_x \quad on \quad \bar{S}_2 \\ &v=\hat{v} \quad on \quad \bar{S}_1 \quad \frac{1}{\mathrm{Re}}(\frac{\partial u}{\partial y}+\frac{\partial v}{\partial x}).n_x+(p+\frac{2}{\mathrm{Re}}\frac{\partial v}{\partial y}).n_y=\hat{c}_y \quad on \quad \bar{S}_2 \end{aligned} \tag{5}$$

3 FREE SURFACE FORMULATION

On a fluid surface, government equation is:

$$\bar{F}=\bar{h}(x,t)+\bar{d}-\bar{y}=0 \quad on \quad \bar{S}_2 \tag{6}$$

Where h is the position of the free surface. The kinematic condition associated with the fluid free surface can be defined as:

$$\frac{D\bar{F}}{D\bar{t}}=0 \tag{7}$$

Using Arbitrary Lagrangian-Eulerian definition and the dimensionless form of the free surface kinematic, equation Eq. 7 can be written as:

$$\frac{\partial h}{\partial t}\Big|_{\xi,\eta}+(u-w_u)\frac{\partial h}{\partial x}-v=0 \tag{8}$$

4 TRANSFORMATION OF THE BASIC EQUATIONS INTO THE MAPPED COORDINATE SYSTEM

The computation of the propagation of free surfaces involves computational boundaries that do not coincide with coordinate lines in physical space. For the finite element method, such problem requires a complicated interpolation function on the local grid lines which results in the local loss of accuracy in the computational solution. Such difficulties require a mapping or transformation from physical space to a generalized space. This mapping transforms the wave propagation model from the physical domain, (x, y) to a computational domain (ξ,η). The use of generalized coordinates implies that a distorted region in physical space is mapped into a rectangular region in the generalized coordinate space, where the unknown interface coincides with a coordinate. Referring to the physical and computational meshes the following mapping, can be established.

$$x = \sum_{i=1}^{3} (\xi + h\alpha_i) F_i(\eta)$$
$$y = \eta(1+h) + (1-\eta)\left[(\xi_i - \xi_{i-1}) tg\beta_{i-1} + \sum_{j=2}^{i-1} \left[(\xi_j - \xi_{j-1}) tg\beta_{j-1} \right] \right] \quad (9)$$

And for pressure and velocity are:

$$p = (1-\eta)\left[1 - (\xi_i - \xi_{i-1}) tg\beta_{i-1} + \sum_{j=2}^{i-1} \left[(\xi_j - \xi_{j-1}) tg\beta_{j-1} \right] \right] \quad (10)$$

$$u = U_1 / \left[1 - (\xi_i - \xi_{i-1}) tg\beta_{i-1} + \sum_{j=2}^{i-1} \left[(\xi_j - \xi_{j-1}) tg\beta_{j-1} \right] \right] \quad (11)$$

where ξ_j and β_j are the initial point and slope of each bed line respectively and U_1 is the flow initial velocity. The function $F_i(\eta)$ is interpolation function. Employing three point interpolations, we have:

$$F_1(\eta) = 1 - 3\eta + 2\eta^2$$
$$F_2(\eta) = 4\eta - 4\eta^2 \quad (12)$$
$$F_3(\eta) = -\eta + 2\eta^2$$

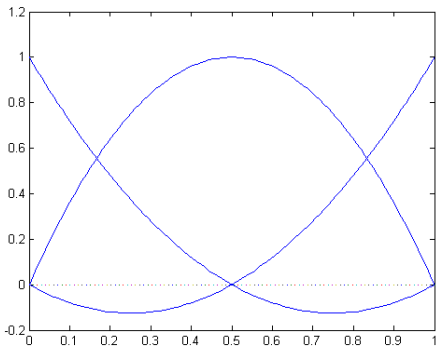

Figure 2. Three point interpolation function

The arbitrary Lagrangian Eulerian description is examined where the spatial coordinates are moving with the velocity and the computation is done in the reference coordinate system ξ and η. This algorithm is employed in free surface modelling over sloping beaches, where the evolution occurs over bathymetry topography, and over constant depth regions. Different types of α_i values are provided and depending on the nature of the problem. To coincide physical and computational boundary, the α_i values are considered to be a fifth order polynomial function of ξ as followed:

$$\alpha_i = \frac{b}{\varepsilon^3 l^5 (1-\varepsilon)^3} [2(\xi - \xi_0)^5 (2\varepsilon - 1) + l(\xi - \xi_0)^4 (4 - 5\varepsilon - 5\varepsilon^2 + 2l^2 (\xi - \xi_0)^3 (-1 - \varepsilon + 5\varepsilon^2) + l^3 \varepsilon (\xi - \xi_0)^2 (3 - 5\varepsilon)] \quad (13)$$

Definitions of b,ε, l and ξ_0 are illustrated in Figure 3.

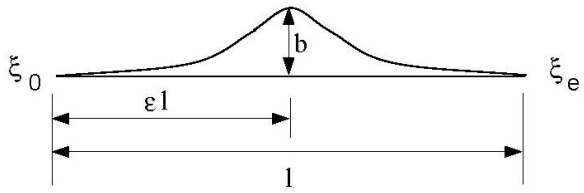

Figure 3. Definition of parameters in α_i function.

Spatial discretization of partial differential equations in the numerical model is based on a Galerkin finite element

method. This method is implemented using the weighted residual variation method for solution within each element. Using standard linear shape functions for a rectangular element in natural coordinate system, the velocity, pressure and correction potential fields within the element are interpolated in terms of their nodal values as follows:

$$u = \psi_\alpha u_\alpha \quad v = \psi_\alpha v_\alpha \quad p = \psi_\alpha p_\alpha \quad \phi = \psi_\alpha \phi_\alpha \quad h = \psi_{\alpha s} h_\alpha \tag{14}$$

Where ψ_α is the interpolation function and u, v, ϕ, h represent the nodal values at the node of the j^{th} element. ϕ is a scalar which is referred to as the correction potential base on the Fractional step method presented by Hayashi and Hatanaka(Hayashi et al., 1991). By dividing the total time *t* into a number of short time increments *Δt*, the equations of motion, continuity and kinematic boundary condition can be discretized into:

$$\begin{aligned} & M_{\alpha\beta} \mid J^{-1} \mid^n \tilde{u}_{i\beta}{}^{n+1} = M_{\alpha\beta} \mid J^{-1} \mid^n u_{i\beta}{}^n - \frac{\Delta t}{\mathrm{Re}}\left[(\frac{2}{j}\delta_{i,1} + j\delta_{i,2}) \xi^n_{k,j} \xi^n_{l,j} M_{\alpha k \beta l} \right] \mid J^{-1} \mid^n u_{i\beta}{}^n \\ & - \frac{\Delta t}{\mathrm{Re}} \xi^n_{l,1} \xi^n_{j,2} (\delta_{i,1} M_{\alpha j \beta l} u^n_{2\beta} + \delta_{i,2} M_{\alpha l \beta j} u^n_{1\beta}) \mid J^{-1} \mid^n - \Delta t \left[\xi^n_{l,j} M_{\alpha\beta\beta l} (u^n_{j\beta} - w^n_{uj\beta}) \right] \mid J^{-1} \mid^n u^n_{i\beta} \\ & + \Delta t \xi^n_{j,i} M_{\alpha j \beta} \mid J^{-1} \mid^n p_\beta{}^n + \sum\nolimits^{\eta}_{\xi_i} \end{aligned} \tag{15}$$

Where:

$$\begin{aligned} \sum\nolimits^{\eta}_{\xi_i} = & \left(- p_\beta{}^n H_{\alpha\beta} + \frac{2}{\mathrm{Re}} \xi^n_{j,i} H_{\alpha\beta j} u_{i\beta}{}^n \right) \left[\left(x^n_{2,2} n_{\xi 1} - x^n_{2,1} n_{\xi 2} \right) \delta_{i,1} + \left(x^n_{1,2} n_{\xi 1} - x^n_{1,1} n_{\xi 2} \right) \delta_{i,2} \right] \\ & + \frac{1}{\mathrm{Re}} \left(\xi^n_{j,2} H_{\alpha\beta j} u^n_{1\beta} + \xi^n_{j,1} H_{\alpha\beta j} u^n_{2\beta} \right) \left[\left(x^n_{2,2} n_{\xi 1} - x^n_{2,1} n_{\xi 2} \right) \delta_{i,2} + \left(x^n_{1,2} n_{\xi 1} - x^n_{1,1} n_{\xi 2} \right) \delta_{i,1} \right] \end{aligned} \tag{16}$$

$$\left(\xi^{n+1}_{l,j} \right)^2 M_{\alpha l \beta l} + \xi^{n+1}_{l,j} \xi^{n+1}_{2,l} \left(M_{\alpha 1 \beta 2} + M_{\alpha 2 \beta 1} \right) \mid J^{-1} \mid^{n+1} \phi_\beta = \xi^{n+1}_{j,l} M_{\alpha\beta j} \mid J^{-1} \mid^{n+1} u_{l\beta}{}^{n+1} + \Phi^{n+1}_s \tag{17}$$

Where

$$\Phi^{n+1}_s = \xi^n_{j,i} H_{\alpha\beta j} \phi^{n+1}_\beta \left[\left(x^{n+1}_{2,2} n_{\xi 1} - x^{n+1}_{2,1} n_{\xi 2} \right) \delta_{1,k} + \left(x^{n+1}_{1,2} n_{\xi 1} - x^{n+1}_{1,1} n_{\xi 2} \right) \delta_{2,k} \right] \tag{18}$$

$$M_{\alpha\beta} u^{n+1}_{i\beta} = M_{\alpha\beta} \tilde{u}^{n+1}_{i\beta} + \xi^{n+1}_{j,i} M_{\alpha\beta} \phi_\beta \tag{19}$$

$$M_{\alpha\beta} \mid J^{-1} \mid^{n+1} p^{n+1}_\beta = M_{\alpha\beta} \mid J^{-1} \mid^{n+1} p^n_\beta - \frac{1}{\Delta t} M_{\alpha\beta} \mid J^{-1} \mid^{n+1} \phi_\beta \tag{20}$$

$$H_{\alpha\beta} \mid J^{-1} \mid^{n+1} h^{n+1}_\beta = H_{\alpha\beta} \mid J^{-1} \mid^{n+1} h^n_\beta + \Delta t \left(H_{\alpha\beta} \mid J^{-1} \mid^{n+1} u^n_{2\beta} - \xi^n_{j,1} H_{\alpha\beta\beta j} \left(u^{n+1}_{1\beta} - w^{n+1}_{uj\beta} \right) \right) \mid J^{-1} \mid^{n+1} h^n_\beta \tag{21}$$

Note that due to the complexity, the equations are written in the mapped domain, using indicial notation. Change of the indices is as:

$$\{ i = 1,2 \ \ [k = 1,2 \ \ (l = 1,2 \quad j = 1,2)] \} \tag{22}$$

Here $\sum\nolimits^{\eta}_{\xi_i}$ and Φ^{n+1}_s are boundary integrals, created in week formulations of governing equations, ξ_i is the reference coordinate system ($\xi_1 = \xi$ and $\xi_2 = \eta$ direction), $\mid J^{-1} \mid$ is the Jacobian inverse of transformation matrix and the following definitions are for the consistent mass matrix obtained from analytical integration used to write the above equations.

$$\begin{array}{lll} M_\alpha = \int_V \psi_\alpha dV & M_{\alpha\beta 1} = \int_v \frac{\partial \psi_\alpha}{\partial \xi} \psi_\beta dV & H_{\alpha\beta} = \int_S \psi_\alpha \psi_\beta dS \\ M_{\alpha\beta} = \int_V \psi_\alpha \psi_\beta dV & M_{\alpha\beta 2} = \int_V \psi_\alpha \frac{\partial \psi_\beta}{\partial \eta} dV & H_{\alpha\beta 1} = \int_S \psi_\alpha \frac{\partial \psi_\beta}{\partial \xi} dS \\ M_{\alpha 1 \beta 1} = \int_V \frac{\partial \psi_\alpha}{\partial \xi} \frac{\partial \psi_\beta}{\partial \xi} dV & M_{\alpha\beta\beta 1} = \int_V \psi_\alpha \psi_\beta \frac{\partial \psi_\beta}{\partial \xi} dV & H_{\alpha\beta 2} = \int_s \psi_\alpha \frac{\partial \psi_\beta}{\partial \eta} dS \\ M_{\alpha 1 \beta 2} = \int_V \frac{\partial \psi_\alpha}{\partial \xi} \frac{\partial \psi_\beta}{\partial \eta} dV & M_{\alpha\beta\beta 2} = \int_V \psi_\alpha \psi_\beta \frac{\partial \psi_\beta}{\partial \eta} dV & H_{\alpha\beta\beta 1} = \int_S \psi_\alpha \psi_\beta \frac{\partial \psi_\beta}{\partial \xi} dS \\ M_{\alpha 2 \beta 1} = \int_V \frac{\partial \psi_\alpha}{\partial \eta} \frac{\partial \psi_\beta}{\partial \xi} dV & & H_{\alpha\beta\beta 2} = \int_S \psi_\alpha \psi_\beta \frac{\partial \psi_\beta}{\partial \eta} dS \end{array} \tag{23}$$

It should be noted that all of the derivations are with respect to ξ_i .

Results

For modeling with Navier-Stokes equations, solitary wave length and wave height are 10 m and 0.4 m respectively, and the physical domain discrete to Δx=Δy=0.125m in space and Δt=0.01 Sec in time as shown in Figure 4.

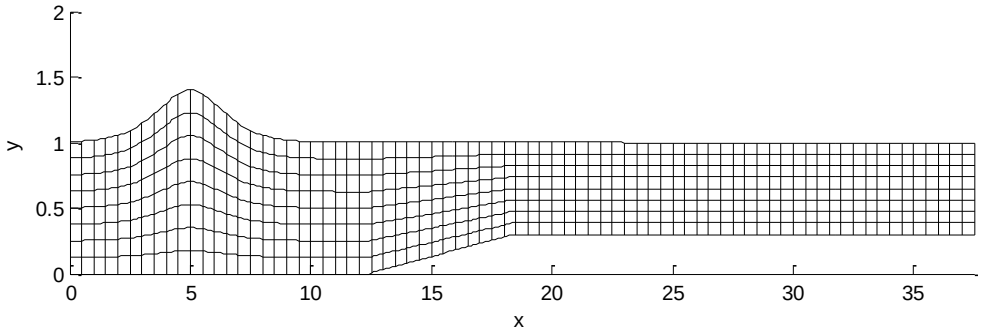

Figure 4. Mesh area and discretization of physical domain for model (t=0.0 Sec)

To comparison between the experimental and numerical data, horizontal (u) and vertical (v) velocity in a solitary wave in this model with experimental model of Grilli et al (Grilli, Losada, & Martin, 1994) at three locations have been compared in Figure 5. Experiments were conducted in the 40 m long, 2 m wide, and 2 m high wave flume and solitary waves were generated using a piston wavemaker. Also the normalized amplitude of the free surface profile of solitary wave *H/d*=0.28 for different timeon bed rises with slope 25%, have been compared in Figure 6. These comparisions show appropriate coinside between this numerical model with experimental data and this model can be used on milder slopes.

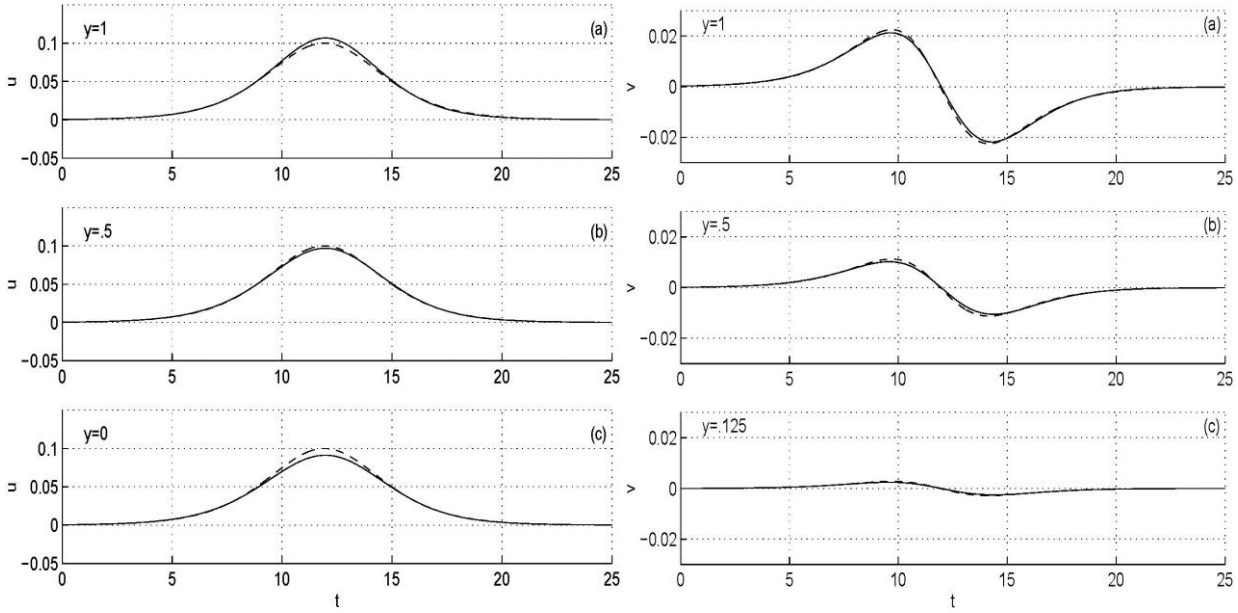

Figure 5. Comparison of horizontal (u) and vertical (v) velocity in a solitary wave in this model with experimental model at three locations. solid line is the present numerical solution; dash line is the experimental data on bed rises

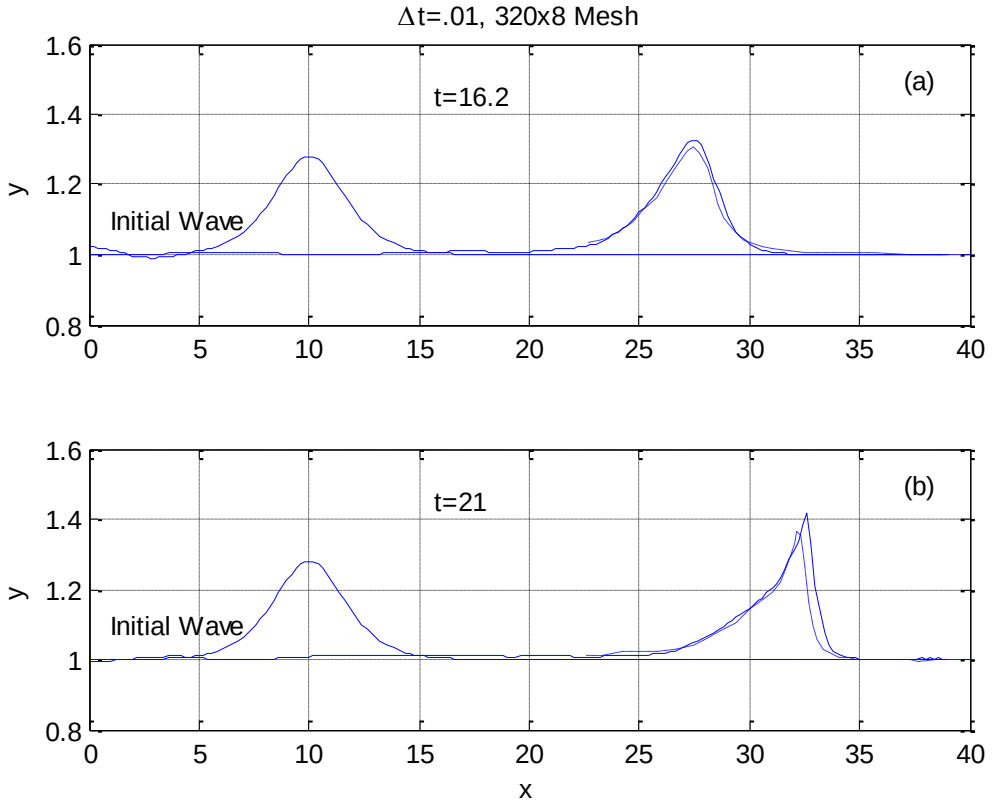

Figure 6. Comparison digram showing the normalizedamplitude of the free surface profile of solitary wave *H/d* = .28for different time: (a) t=16, (b) t=21; solid line is the present numerical solution; dash line is the experimental data on bed rises with slope 25%.

Figure 7 to ~~Figure 8Figure 7 to~~ Figure 11 shows solitary wave profile crossing on bed rises with slope 5%, 10%, 15%, 20% and 25%. Comparison between results shows that the wave height increase and wave length decrease through slope rising.

For better showing the capability of this numerical method and the FORTRAN code that is prepared, some output is presented in Figure 12 to Figure 16. In each figure, wave height (H), horizontal velocity (u) and vertical velocity (v) are shown in times of 0.0 and 15.0 second after flow entry with different slopes.

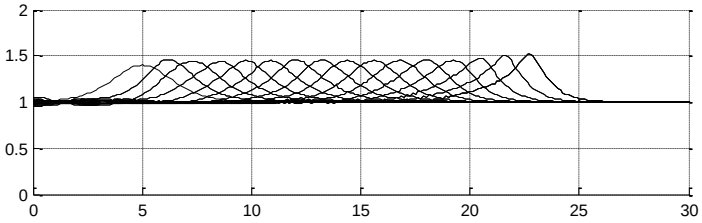

Figure 7. Solitary wave profile of height (H) crossing on bed rises with slope 5%.

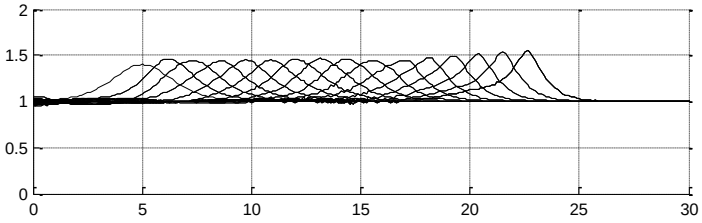

Figure 8. Solitary wave profile of height (H) crossing on bed rises with slope 10%.

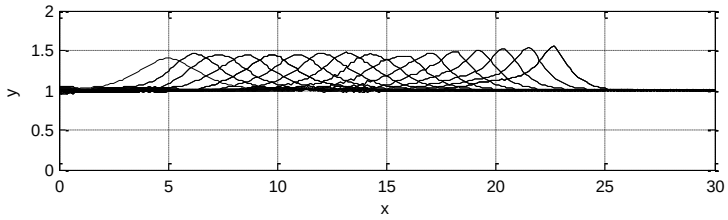

Figure 9. Solitary wave profile of height (H) crossing on bed rises with slope 15%.

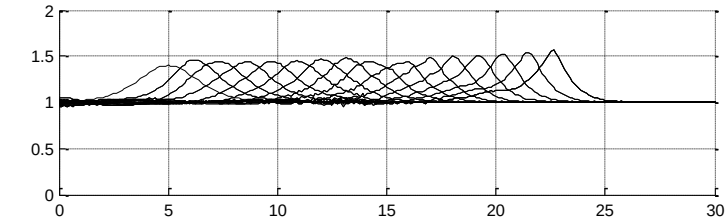

Figure 10. Solitary wave profile of height (H) crossing on bed rises with slope 20%.

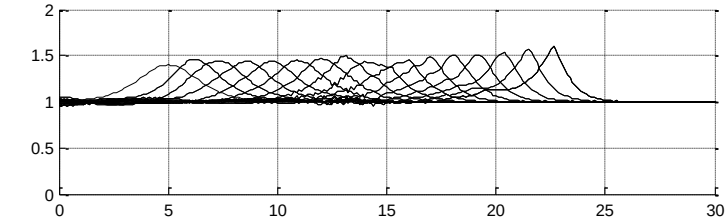

Figure 11. Solitary wave profile of height (H) crossing on bed rises with slope 25%.

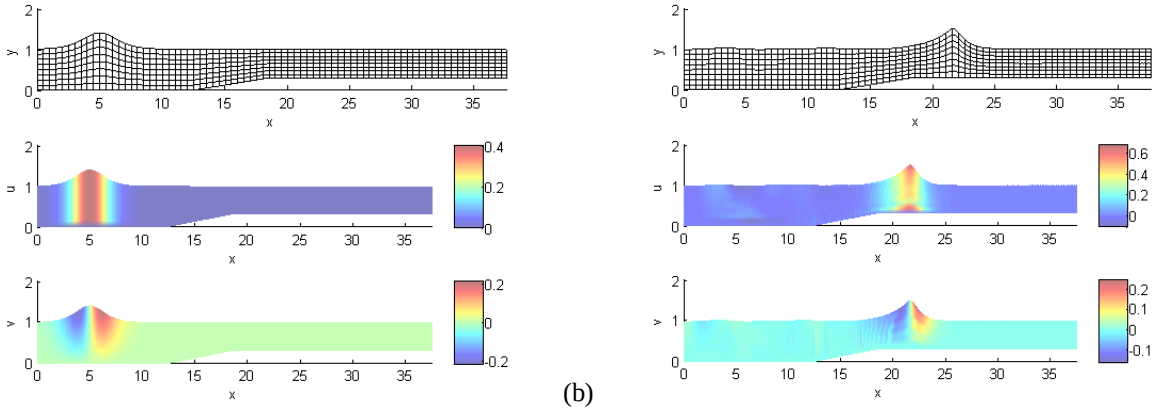

(a) (b)

Figure 12. Wave height, horizontal and vertical velocity on bed rise with 5% slope in (a): t=0, (b): t=15 Sec.

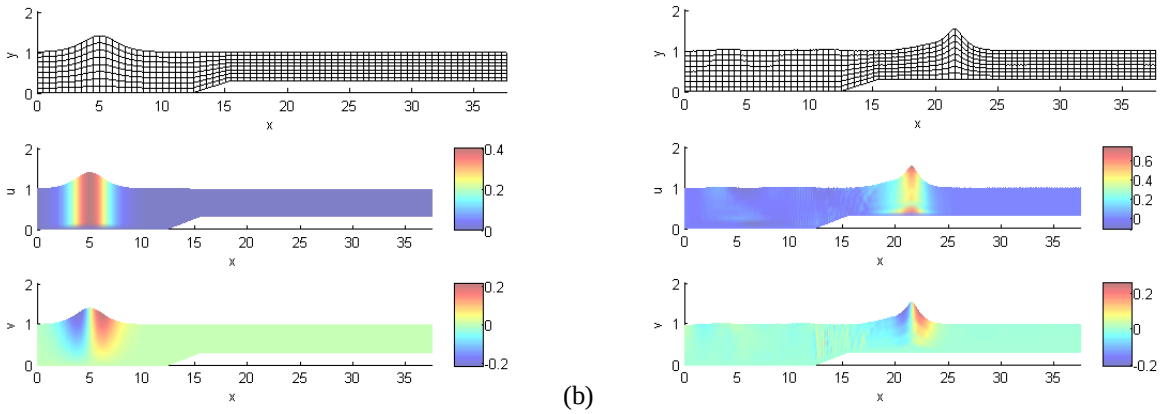

(a) (b)

Figure 13. Wave height, horizontal and vertical velocity on bed rise with 10% slope in (a): t=0, (b): t=15 Sec.

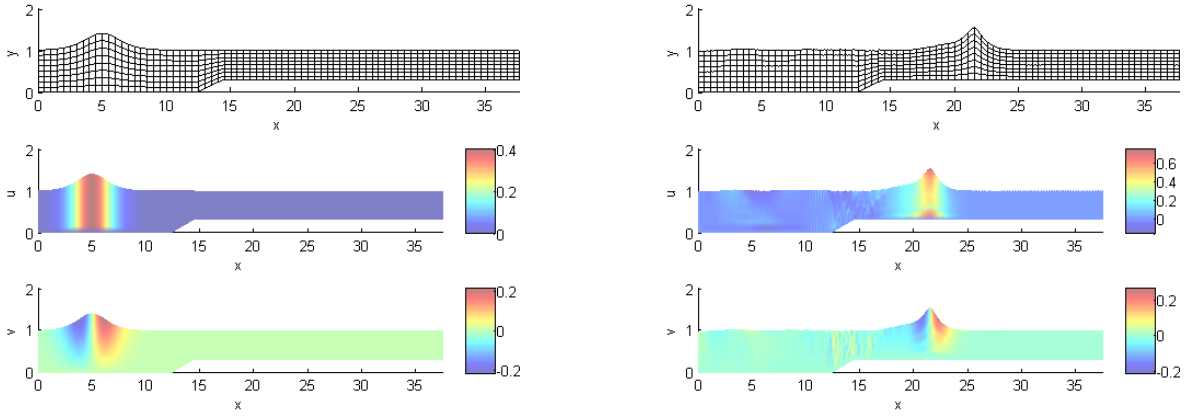

(a) **(b)**

Figure 14. Wave height, horizontal and vertical velocity on bed rise with 15% slope in (a): t=0, (b): t=15 Sec.

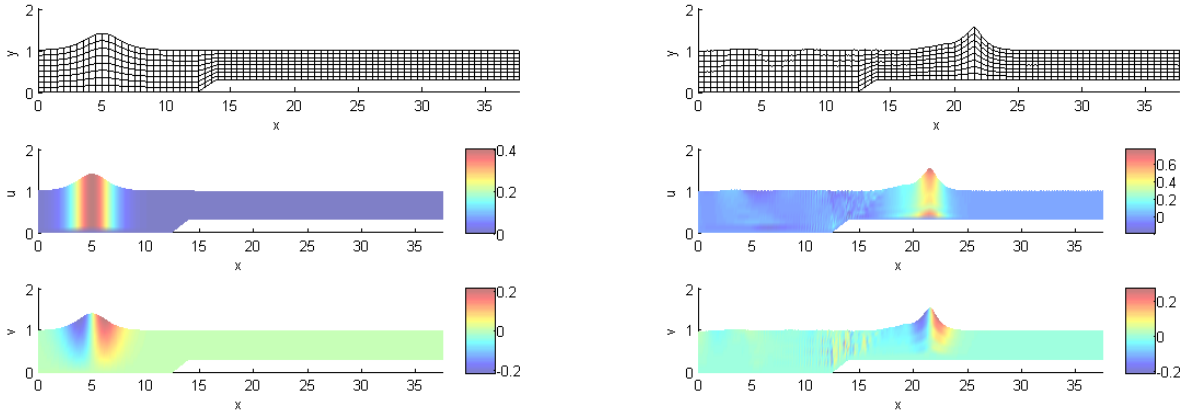

(a) **(b)**

Figure 15. Wave height, horizontal and vertical velocity on bed rise with 20% slope in (a): t=0, (b): t=15 Sec.

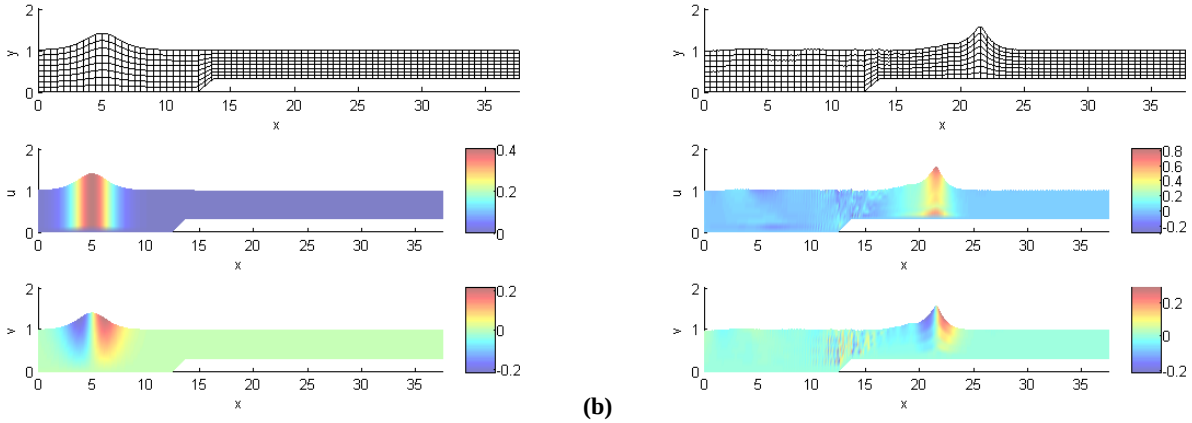

(a) **(b)**

Figure 16. Wave height, horizontal and vertical velocity on bed rise with 25% slope in (a): t=0, (b): t=15 Sec.

5 CONCLUSION

This numerical approach is very suitable for solving Navier Stokes with keep the accurate of calculating. This approach has good results and shows that the wave height increase and wave length decrease through slope rising. This approach can be used to model any kind of submerged breakwater to protect the coastal region against tsunamis. With mapping techniques and arbitrary Lagrangian-Eulerian approach, the model shows the solitary wave cross over bed rise. The reason

for the selecting of arbitrary Lagrangian-Eulerian description for modelling of flow is force the model to cope with several of free surface and the model can be employed in any geometry, under complicated boundary conditions without any additional computational effort. The model can be employed in any geometry, under complicated boundary conditions, and with arbitrary bathymetry, without any additional computational effort. It is almost a general method to handle different aspects of coastal hydrodynamics problems. Another advantage of the present study is that no smoothing or artificial viscosity is applied. The model's convergence is satisfactory and in contrast to most of the other methods. The developed techniques could easily be extended to analyze many other free surface problems such as wave breaker and waves interaction.

REFERENCES

Christou, M., Swana, C., & Gudmestad, O. T. (2008). The interaction of surface water waves with submerged breakwaters. *Coastal Engineering, 55*, 945–958.

Cooker, M. J., Weidman, P. D., & Bale, D. S. (1997). Reflection of a high-amplitude solitary wave at a vertical wall. *J. Fluid Mech, 342*(141).

Dolatshahi P., M., & Wellford, C. L. (1995). *Finite element methods for viscous free surface fluids including breaking and non-breaking waves.*, University of Southern California California.

Dommermuth, D. G., Yue, D. K. P., Lin, W. M., Rapp, R. J., Chan, E. S., & Melville, W. K. (1988). Deep-water plunging breakers: A comparison between potential theory and experiments. *J. Fluid Mech, 189*, 423–442.

Gaston, L., & Kamara, A. (2000). Arbitrary Lagrangian-Eulerian finite element approach to non-steady state turbulent fluid flow with application to mould filling in casting. *International Journal for Numerical Methods in Fluids., 34*(4), 341-369.

Grilli, S. T., Losada, M. A., & Martin, F. (1994). Characteristics of Solitary Wave Breaking Induced by Breakwaters. *Journal of Waterway Port Coastal and Ocean Engineering, 120*(1), 74-92.

Hayashi, M., Hatanaka, K., & Kawahara, M. (1991). Lagrangian Finite Element Method for Free Surface Navier-Stokes Flow Using Fractional Step Methods. *Int Journal for Numerical Methods in Fluids., 13*, 805-840.

Irtem, E., Seyfioglu, E., & Kabdasli, S. (2011). Experimental Investigation on the Effects of Submerged Breakwaters on Tsunami Run-up Height. *Journal of Coastal Research., Special Issue 64*, 516-520.

Kim, P. L., Liu, J. A., & Liggett, S. K. (1983). Boundary Integral Equation Solutions for Solitary Wave Generation, Propagation and Run-Up. *Coastal Engineering., 7*, 299-317.

Lemos, C. M. (1992). A simple numerical technique for turbulent flows with free surfaces. *International Journal of Numerical Methods in Fluids, 15*, 127– 146.

Lo, D. C., & Young, D. L. (2004). Arbitrary Lagrangian-Eulerian finite element analysis of free surface flow using a velocity-vorticity formulation. *J of Comp Physics., 195*, 175-201.

Ramaswamy, B., & Kawahara, M. (1987). Arbitrary Lagrangian-Eulerian Finite Element Method for Un¬steady Convective Incompressible Viscous Free Surface Fluid Flow. *International Journal for Numerical Methods in Fluids., 7*, 1053-1075.

Wellford, C. L., & Ganaba, T. H. (1981). A Finite Element Method with a Hybrid Lagrangian Line for Fluid Mechanics Problems Involving Large Free Surface Motion. *Int. Journal for Numerical Methods in Engineering., 17*, 1201-1231.

Zhou, J. G., & Stansby, P. K. (1998). An arbitrary Lagrangian-Eulerian (ALE) model with non-hydrostatic pressure for shallow water flows. *Computer Methods in Applied Mechanics and Engineering., 178*, 199-214.